

# Precollision and postcollision electron-electron correlation effects for intermediate-energy proton-impact ionization of helium

M. Foster, J. L. Peacher, M. Schulz, A. Hasan, and D. H. Madison

*Laboratory for Atomic, Molecular and Optical Research, Physics Department, University of Missouri-Rolla, Rolla, Missouri 65409-0640, USA*

(Received 11 October 2005; published 16 December 2005)

We report fully differential cross sections (FDCS) for the single ionization of helium by a 75 keV incident energy proton. Previous three-body distorted wave (3DW) calculations for this collision system are in poor agreement with the absolute magnitude of the experimental measurements. The 3DW approximation treats the four-body problem as an effective three-body problem in which the passive electron does not participate in the collision. We have developed a full four-body approach in which the passive electron fully participates in the collision. It will be shown that the FDCS is very sensitive to the treatment of the passive electron-ejected electron interaction. Results of our full four-body approach will be compared with recent absolute experimental measurements.

DOI: [10.1103/PhysRevA.72.062708](https://doi.org/10.1103/PhysRevA.72.062708) PACS number(s): 03.67.Hk, 34.10.+x, 03.65.Ud, 34.85.+x, 03.65.Nk, 34.50.Fa

## I. INTRODUCTION

Single ionization of atomic targets by charged particle impact has been studied for decades. Although spectacular progress in the theoretical description of the fully differential angular distributions of the ejected electrons was achieved even for the most simple target atom (hydrogen) some discrepancies between experiment and theory remain [1–5]. The theoretical models vary from numerical solutions of the Schrödinger equation to perturbative models that use asymptotically correct final-state wave functions. Unfortunately, all of the theoretical models have some shortcomings. Consequently, the search for one theoretical model that can accurately predict the physics of charged particle impact ionization of hydrogen at any collision energy and any type of projectile continues.

A helium target is interesting since it represents the simplest system containing passive electrons. Treating the passive electrons properly represents a formidable challenge for theory. As a result, their role in the ionization process is usually treated by using approximations, the validity of which not always being obvious. The standard approximation used for single ionization of a helium target is to model the four body problem (projectile, target nucleus, and two atomic electrons) as an effective three-body problem, i.e., projectile, active electron, and residual target ion. In a three-body model, the role of the passive electron is to partially screen the nucleus of the ion. The simplest treatment of this screening is to approximate the ion as an effective charge. A better treatment is to use a Hartree-Fock potential for the ion in which case the passive electron provides no screening near the nucleus and full screening when the ejected electron is far from the nucleus. Consequently, for ionization of helium, the ejected electron would “see” a net charge of +2 close to the nucleus and a net charge of +1 at large distance.

For the scattering plane (spanned by the initial and final projectile momenta  $\mathbf{k}_0$  and  $\mathbf{k}_1$ , respectively), the three-body distorted wave (3DW) model has yielded good agreement with fully differential cross sections (FDCS) experiments for

$\text{C}^{6+}$  ionization of helium [6,7]. However, serious discrepancies were found outside the scattering plane [8]. Furthermore, very poor agreement with experiment was found for ionization of helium by impact of highly charged gold ions [9–12]. For the single ionization of helium by  $\text{Au}^{q+}$  ( $q=24, 53$ ), the 3DW FDCS were nearly a factor of 20 smaller than the experimental results. Also the experimental data was strongly peaked in the forward direction, i.e., along the beam axis. The forward peak was thought to be explained by the highly charged gold ion “dragging” the ionized electron forward. It was suggested by Rodriguez *et al.* [10] and later by Foster *et al.* [11] that a four-body treatment might improve the agreement in magnitude between theory and experiment. It is difficult to determine if the failure of the theory is due to the three-body modeling or the exclusion of physical effects not contained within the model, such as polarization of the helium atom.

More recently, experiments have been performed for single ionization of helium by 75 keV proton impact [13]. Maydanyuk *et al.* [13] compared the experimental data with the 3DW results. They found that the overall shape of the 3DW cross sections were in good agreement with the data except for some small shifts in the binary peaks. However, on an absolute scale, there were significant discrepancies. The 3DW model was about a factor of 4 too large relative to the experimental data. In fact, the much simpler first-Born-approximation-Hartree-Fock (FBAHF) gave results closer to the magnitude of the experimental data. The important difference between the 3DW model and the FBAHF calculation is that the 3DW approach includes the interactions between the projectile and the residual target ion as well as with the ejected electron in the initial and final-state wave function for the projectile whereas the FBAHF calculation does not. The FDCS results for 75 keV proton impact ionization of helium are shown in Fig. 1 for an ejected-electron energy  $E_e=5.5$  eV and four different momentum transfer values  $|\mathbf{q}|$  where  $\mathbf{q}=\mathbf{k}_0-\mathbf{k}_1$  ( $|\mathbf{q}|=0.64, 0.67, 0.76, \text{ and } 0.97$  a.u.). The different momentum transfer values correspond to increasing proton scattering angles, i.e.,  $\theta_p=6.5, 6.8, 7.7, \text{ and}$

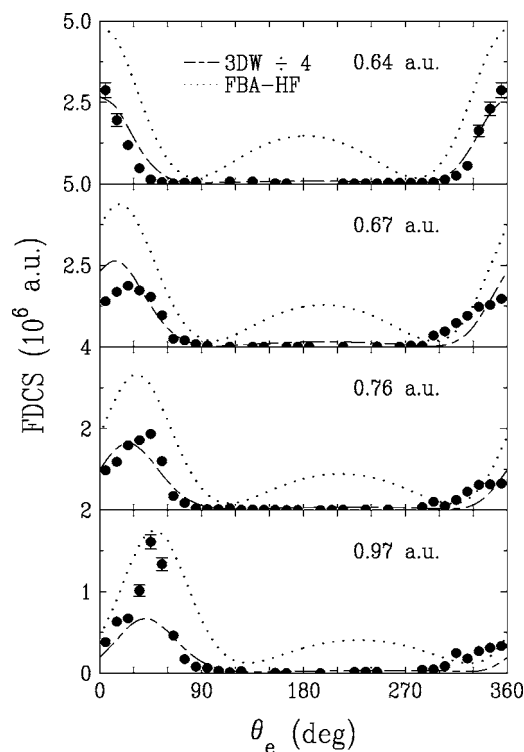


FIG. 1. Fully differential cross sections for 75 keV  $p^+$  impact ionization of helium in the scattering plane. All of the experimental data are absolute values in the center of mass frame. The ejected electron energy  $E_e$  is 5.5 eV and the magnitude of the momentum transfer,  $|\mathbf{q}|$ , is indicated in each part of the figure. The emission angle  $\theta_e$  of the ejected electron in the scattering plane is measured clockwise from the beam direction. The solid circles are the absolute measurements and the theoretical curves: dotted line FBA-HF, and long-dash short-dashed line 3DW model divided by a factor of 4.

9.9 m deg, respectively. A standard rating of the strength of the perturbation is the ratio between projectile's charge and its velocity  $z_p/v_p$  and perturbation theory results should become better as this ratio decreases. For Fig. 1,  $z_p/v_p$  is approximately 0.7, which is approximately the same ratio as 2 MeV/u  $C^{6+}$  single ionization of helium [11]. Since the collision strengths are the same, one might expect similar agreement between experiment and theory. However, instead of the poor agreement seen in Fig. 1, very good agreement between experiment and theory was found for 2 MeV/u  $C^{6+}$  ionization of helium in the scattering plane.

The 3DW model predicted FDSC for the 2 MeV/u  $C^{6+}$  single ionization of helium that agreed with experiment both in shape and magnitude. The ejected electron energies and momentum transfer values were approximately the same for both the proton and carbon collisions. The important question that remains is—what is different in the physics between the collisions for  $C^{6+}$  impact and the collisions for  $p^+$  impact ionization of helium? One possible difference is the relative velocities between the final-state projectile and the ejected electron. The magnitude of the relative velocity for the proton case is 1.1 a.u. as opposed to 8.2 a.u. for the 2 MeV/u  $C^{6+}$  case. As a result, the final-state postcollision interaction (PCI) should play a more important role for proton impact

ionization of helium. Another possible difference is the importance of the passive electron. If the passive electron plays an important role, it would probably be stronger for proton impact than  $C^{6+}$  impact ionization because the capture channel is much more likely for proton impact ionization than the  $C^{6+}$  impact ionization. Along with testing the approximations that the 3DW model makes for the effective three-body geometry, we will examine correlation effects between the passive and active electrons in both the initial and final wave functions in this paper.

For the process of double ionization of a helium atom, there have been several studies of the importance of correlation in the initial-state atomic helium wave function [14–16], and it has been found that the FDSC varies greatly depending on the choice for the initial-state helium wave function. Many choices for the helium wave function are available and each has strengths and weaknesses. The well-known Hylleraas wave function, for example, can be chosen such that it yields the ground state energy of the helium atom accurately to many significant digits. However, the Hylleraas wave function does not satisfy the Kato cusp condition which is a requirement for the wave function when the two electrons are at the same location. The Pluvinaige wave function, on the other hand, is a relatively simple wave function that does satisfy the Kato cusp condition. The ground-state energy predicted by the Pluvinaige wave function is only accurate to about 2% of the actual experimental value. However, if the behavior of the wave function when the two electrons are close together is more important than the total energy, it could be that it would be better to use the Pluvinaige wave function than the Hylleraas wave function. For the FDSC for double ionization of helium, the Pluvinaige wave function gives better agreement with the absolute experimental results than the use of a Hylleraas wave function [14,17]. In this paper, we will examine the effects of using a different initial state as well as final-state wave functions for single ionization of helium by protons using both three-body and four-body models. Atomic units will be used throughout unless otherwise stated. Also, the experimental results and theoretical calculations will be given in the center-of-mass frame in the equations and in the figures.

## II. THEORY

The details of the 3DW model discussed above have been given in previous papers [11, and references therein], so only the necessary additional features for describing the four-body model will be presented here. The fully differential cross section (FDSC) is a fivefold differential cross section (four angles and one energy). Combining the differentials in the polar and azimuthal angles to a single differential in solid angle  $d\Omega = \sin\theta d\theta d\Phi$ , it can also be expressed as a triply differential cross section in the center of mass system, and is given by [18–20]

$$\frac{d^3\sigma}{d\Omega_p d\Omega_e dE_e} = (2\pi)^{-5} \mu_{Ie} \mu_{PA}^2 \frac{k_1 k_2}{k_0} |T_{fi}|^2. \quad (1)$$

The reduced mass of the helium-ion-electron subsystem is  $\mu_{Ie}$  and the reduced mass of the projectile-target atom system

is  $\mu_{PA}$ . The initial and final momenta of the projectile are  $\mathbf{k}_0$  and  $\mathbf{k}_1$ , the ejected-electron's energy and momentum are given by  $E_e$  and  $\mathbf{k}_2$ , respectively, and all continuum waves are asymptotically normalized to plane waves. The solid angles for the projectile and the ejected electron are given by  $\Omega_p$  and  $\Omega_e$ , respectively. If  $r_3$  is the coordinate for the passive electron, the four-body transition matrix (T-matrix) for the ionization of helium is

$$T_{fi} = \langle \chi_f^-(r_1, r_2, r_3) | H - H_0 | \psi_i(r_1, r_2, r_3) \rangle. \quad (2)$$

Here  $H$  is the full four-body Hamiltonian for the proton-helium system and  $H_0$  is the initial-state asymptotic form of  $H$ . The initial-state wave function for the system  $\psi_i(r_1, r_2, r_3)$  is an eigenfunction of  $H_0$  and  $\chi_f^-(r_1, r_2, r_3)$  is an approximate eigenfunction for  $H$ . The full four-body Hamiltonian  $H$  for the proton-helium system is given by

$$H = -\frac{1}{2\mu_{PA}}\nabla_{\mathbf{r}_1}^2 - \frac{1}{2}\nabla_{\mathbf{r}_2}^2 - \frac{1}{2}\nabla_{\mathbf{r}_3}^2 + \frac{2}{|\mathbf{r}_1|} - \frac{1}{|\mathbf{r}_1 - \mathbf{r}_2|} - \frac{1}{|\mathbf{r}_1 - \mathbf{r}_3|} - \frac{2}{|\mathbf{r}_2|} - \frac{2}{|\mathbf{r}_3|} + \frac{1}{|\mathbf{r}_2 - \mathbf{r}_3|} \quad (3)$$

and  $H_0$  is

$$H_0 = -\frac{1}{2\mu_{PA}}\nabla_{\mathbf{r}_1}^2 - \frac{1}{2}\nabla_{\mathbf{r}_2}^2 - \frac{1}{2}\nabla_{\mathbf{r}_3}^2 - \frac{2}{|\mathbf{r}_2|} - \frac{2}{|\mathbf{r}_3|} + \frac{1}{|\mathbf{r}_2 - \mathbf{r}_3|}. \quad (4)$$

The difference between  $H - H_0 = V_i$  (the initial channel interaction potential) is given by

$$V_i = 2/r_1 - 1/r_{12} - 1/r_{13}. \quad (5)$$

As a result, the T-matrix can be expressed as

$$T_{fi} = \langle \chi_f^-(r_1, r_2, r_3) | V_i | \psi_i(r_1, r_2, r_3) \rangle. \quad (6)$$

### A. Initial-state wave function

In the four-body geometry, the initial-state wave function can vary greatly depending on how the correlation between the two bound electrons is treated. In the independent electron model (IEM) for the helium atom, correlation is ignored in the Hamiltonian and the ground state energy obtained from the resulting wave functions is approximately 37% too low ( $E_{\text{IEM}} \approx -108.8$  eV and  $E_{\text{exp}} \approx -79.0$  eV) [21]. However, when  $1/r_{23}$  is included in the helium wave function (such as a 20-parameter Hylleraas wave function), it is possible to obtain highly accurate ground state energies. Consequently, including the interaction between the two electrons is vital if one wants to model the proper physics of a many electron system such as helium.

One goal of the present paper is to determine the importance of the initial-state and final-state correlation between the passive electron left in the ground state and a continuum electron. To this end, we have performed calculations using three types of correlated initial-state wave functions: a 20-parameter Hylleraas wave function [22,23], the Le Sech wave function [24], and the Pluvillage wave function [25].

As mentioned above, the 20-parameter Hylleraas wave function is considered the benchmark wave function for an isolated helium atom due to the precision of the ground-state energy. However, as stated in the Introduction, the Hylleraas wave function does not satisfy the Kato cusp condition. In order for the cusp condition to be satisfied, the local energy must be a constant as  $r_{23} \rightarrow 0$  [14]. For the Hylleraas wave function, the local energy is infinite as  $r_{23} \rightarrow 0$ . The 20-parameter Hylleraas wave function has the form

$$\phi_H(s, t, u) = N e^{-\lambda s} \sum_{a,b,c} C_{a,b,c} s^a t^b u^c, \quad (7)$$

where  $s = r_2 + r_3$ ,  $t = r_2 - r_3$ , and  $u = r_{23}$  are elliptic coordinates (see Ref. [23] for the specific values of the parameters). The second correlated initial-state wave function tested was the Le Sech wave function. The Le Sech wave function is a three parameter analytic wave function that satisfies the cusp condition requirement and yields the ground-state energy to within three significant digits. The Le Sech wave function used in our calculations has the form

$$\phi_{LS}(r_2, r_3) = N e^{-Z_t r_2} e^{-Z_t r_3} [\cosh(\lambda r_2) + \cosh(\lambda r_3) + b(r_2 - r_3)^2] \times [1 + 0.5 r_{23} e^{-a r_{23}}]. \quad (8)$$

The charge of the nucleus  $Z_t$  is equal to two and the other parameters can be found in Ref. [24]. The third correlated initial-state wave function we tested was the Pluvillage wave function. Although the Pluvillage wave function satisfies the Kato cusp conditions, the ground-state energy of helium is not as accurate as the previous two wave functions ( $\sim 1\%$  off the exact value). The reason we were interested in the Pluvillage wave function lies in the fact that the Pluvillage wave function has a similar structure as the final-state 3DW wave function in that it is also expressed as a product function for the three subsystems of the target atom. For double ionization of helium, the Pluvillage wave function in conjunction with the final-state 3DW wave function yielded much better results than using a more accurate Hylleraas wave function [14]. The Pluvillage wave function used in our model is given by the form

$$\phi(r_2, r_3) = \frac{Z_t^3}{\pi} N(k) e^{-Z_t r_2} e^{-Z_t r_3} e^{ikr_{23}} {}_1F_1(1 - i\mu/k, 2, 2ikr_{23}), \quad (9)$$

here the parameter  $k = 0.41$  a.u. minimizes the ground-state energy,  $N = 0.60337$ , and  ${}_1F_1$  is a confluent hypergeometric function which represents the repulsion between the two atomic electrons.

The initial-state wave function for the projectile-helium system  $\psi_i$  is an eigenfunction of the asymptotic Hamiltonian  $H_0$ . Since the asymptotic Hamiltonian contains no interactions between the projectile and atom,  $\psi_i$  is a product of a plane wave for the projectile and these correlated initial-state wave functions for the helium atom. As a result, the initial-state wave function  $\psi_i$  has the form

$$\psi_i = (2\pi)^{-3/2} \exp(i\mathbf{k}_0 \cdot \mathbf{r}_1) \phi(\mathbf{r}_2, \mathbf{r}_3). \quad (10)$$

### B. Final state wave function

The final-state wave function,  $\chi_f^-(\mathbf{r}_1, \mathbf{r}_2, \mathbf{r}_3)$  for the four-body dynamics will be an extension of the 3DW final-state wave function. The 3DW wave function takes into account the three possible pairs of two-particle interactions for the final state in a three-body system. For a four-body system, there are six pairs of two-body interactions and our final-state four-body wave function will take into account all six pairs on an equal footing. Consequently, we call our final-state four-body wave function the six-distorted-wave (6DW) wave function. The T-matrix in Eq. (6) is now a nine-dimensional numerical integration which we perform using Gauss-Legendre quadratures [26]. The 6DW final-state wave function  $\chi_f^-$  is given by [27–31]:

$$\begin{aligned} \chi_f^- = & (2\pi)^{-3} \exp(i\mathbf{k}_1 \cdot \mathbf{r}_1 + i\mathbf{k}_2 \cdot \mathbf{r}_2) C^-(\eta_1, \mathbf{k}_1, \mathbf{r}_1) C^-(\eta_2, \mathbf{k}_2, \mathbf{r}_2) \\ & \times C^-(\eta_{12}, \mathbf{k}_{12}, \mathbf{r}_{12}) C^-(\eta_{13}, \mathbf{k}_{13}, \mathbf{r}_{13}) C^-(\eta_{23}, \mathbf{k}_{23}, \mathbf{r}_{23}) \psi_{1^2s}(z) \\ & = 2, \mathbf{r}_3). \end{aligned} \quad (11)$$

Here  $C$  is the Coulomb distortion factor defined as

$$C^-(\eta, k, r) = \Gamma(1 - i\eta) \exp(-\pi\eta/2) {}_1F_1(i\eta, 1, -ikr - i\mathbf{k} \cdot \mathbf{r}), \quad (12)$$

where  ${}_1F_1$  is a confluent hypergeometric function and  $\Gamma$  is the gamma function. The Sommerfeld parameters are given by  $\eta_1 = Z_p/v_1$ ,  $\eta_2 = -Z_{\text{He}^+}/v_2$ ,  $\eta_{12} = -Z_p/v_{12}$ ,  $\eta_{13} = -Z_p/v_{13}$ , and  $\eta_{23} = 1/v_{23}$ . The final-state wave function  $\chi_f^-$  takes all six two-particle interactions into account to all orders of perturbation theory.

In Eq. (11), the ionized electron and passive electron are distinguished for simplicity. In the actual calculations, the final-state wave function is properly antisymmetrized.

### III. RESULTS

We have investigated the FDCS for single ionization of helium by impact of 75 keV protons. Since the 6DW calculations are computationally time-consuming, we first examine the importance of the interaction between the passive and active electrons within the first Born approximation (FBA). For this study, the projectile is treated as a plane wave, various different correlated wave functions are used for the initial atomic state, and the 3C wave function is used for the (nucleus, passive-electron, active-electron) system. We will use the following notation—model type (type of initial state, type of final state). For example, FBA (HY, 3C) means a first Born approximation calculation where the initial atomic state is Hylleraas and the final state of the (nucleus, passive-electron, active-electron) system is a 3C wave function.

In Fig. 2, we present FBA FDCS results in the scattering plane using the Hylleraas initial-state [FBA (HY, 3C)—dashed-dotted line] and the Pluvinaige initial-state wave function [FBA (PL, 3C)—bold dashed line]. We have not shown the results using the Le Sech wave function since they were nearly identical to the results using the Hylleraas wave function. For Fig. 2, the ejected electron's energy,  $E_e = 5.5$  eV and the different parts of the figure are for different momentum transfer from the proton varying between 0.64 and 0.97 a.u.

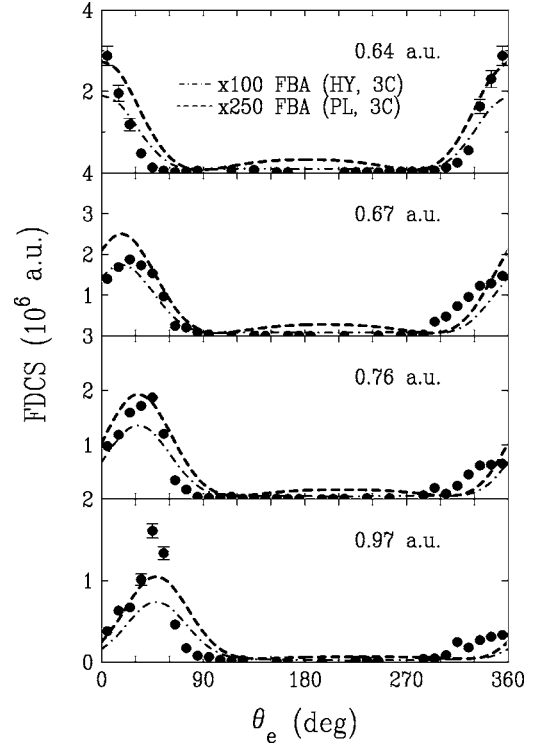


FIG. 2. Same kinematical conditions as Fig. 1, the solid circles are the absolute measurements and the theoretical curves are dashed-dotted line FBA (HY, 3C) model multiplied by a factor of 100, and the dashed line FBA (PL, 3C) model multiplied by a factor of 250.

From Fig. 2 it is seen that the agreement between theory and the shape of the experimental data is satisfactory. However, the absolute magnitudes are factors of 100 and 200 too small whereas the 3DW results of [13] were a factor of 4 too big. Clearly, letting the passive electron play a role in the collision has had an enormous effect on the FDCS. The important question is—what causes this extreme change in the FDCS magnitude results? From Fig. 2, it is also seen that the difference between the Hylleraas and Pluvinaige initial-state wave functions is a factor of 2.5. Consequently, the bulk of the magnitude change has to originate from the final-state interactions. We investigated the importance of the various final-state two-particle interactions and found that the one that causes almost all of the change is the final-state passive-electron continuum-electron interaction. The failure of the present final-state electron-electron correlation is undoubtedly related to the fact that the Coulomb interaction used for the electron-electron subsystem is valid for two electrons in the continuum, not for a bound-electron free-electron interaction. For the process of double ionization of helium, where both electrons are unbound in the final state, the Coulomb interaction used in Eq. (11) yielded excellent agreement between theory and experiment [14–16]. The failure of Eq. (11) for single ionization of helium using four-body geometry lies in the fact that the final-state electron-electron interaction does not take into account the fact that one of the electrons is bound.

We have investigated two different approximations for treating the final-state interaction between a bound and a

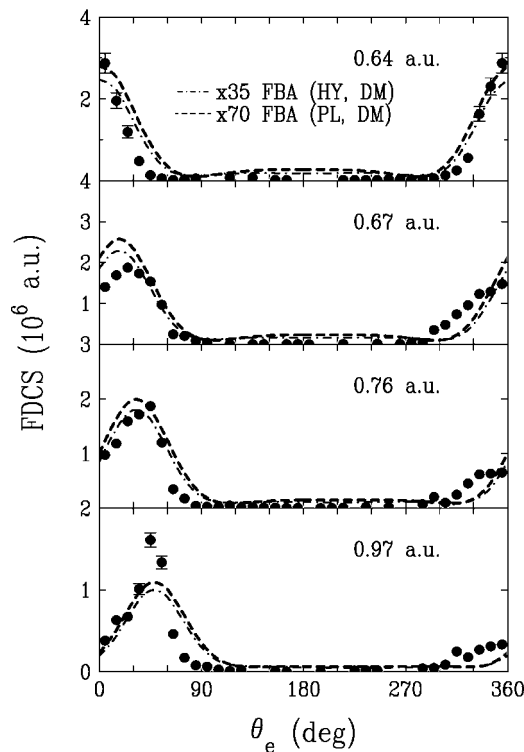


FIG. 3. Same kinematical conditions as Fig. 1, the solid circles are the absolute measurements and the theoretical curves are dashed-dotted line FBA (HY, DM) model multiplied by a factor of 35, and the short-dashed line FBA (PL, DM) model multiplied by a factor of 70.

continuum electron. The first of these approximations will be labeled as the Dewangan mass approximation (DM). For the 3DW initial-state wave function proposed by Dewangan and Bransden, the bound electron is given by the mass of the nucleus [32]. The mass of the bound electron enters into the reduced mass of the electron-electron subsystem. Making the bound electron mass equivalent to the nuclear mass has the net effect of changing the reduced mass  $\mu$  from  $\frac{1}{2}$  to unity in the electron-electron correlations function [33]. Which means that the wave vector  $k_{23}=v_{23}$  in Eq. (11). The results of incorporating the DM into the final-state Coulomb interaction for the passive-electron continuum-electron in the FBA model is shown in Fig. 3. The kinematics for Fig. 3 are the same as the previous figures ( $E_e=5.5$  eV and  $|q|=0.64, 0.67, 0.76,$  and  $0.97$  a.u.). Although the magnitude of the FDCS increased significantly by introducing the DM approximation, the absolute value is still factors of 35 and 70 smaller than the experimental data. Nevertheless, it is intriguing to see that changing the reduced mass of the electron-electron subsystem from 0.5 to 1.0 altered the overall FDCS by factors of nearly 3.

The second approximation we investigated for treating the interaction between a bound electron and a free electron was to use complex effective charges. The idea for using complex charges was first proposed by Crothers and McCarroll [34] in connection with low energy electron-impact excitation of hydrogen. This approximation was later used by Nath *et al.* [35] in their study of simultaneous ionization and excitation

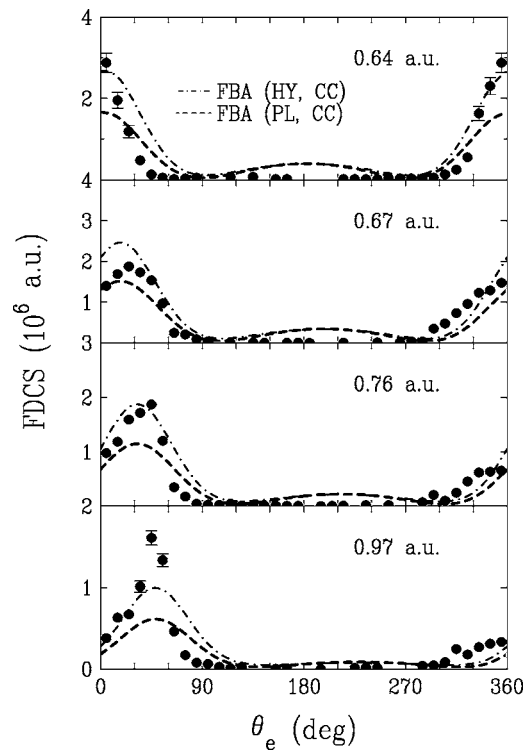


FIG. 4. Same kinematical conditions as Fig. 1, the solid circles are the absolute measurements and the theoretical curves are dashed-dotted line FBA (HY, CC) model, and the dashed line FBA (PL, CC) model.

of helium by electron impact. In this approximation, the passive-electron continuum-electron's Sommerfeld parameter,  $\eta_{23}$ , is modified to  $\eta_{23}=-1/(k_2-i\sqrt{\epsilon_n})$  where  $\epsilon_n$  is the ionization potential (in rydbergs) of the  $n$ th level of the  $\text{He}^+$  ion. We will label the Crothers and McCarroll [34] complex effective charge approximation as CC. The CC results for the FDCS are shown in Fig. 4. Now both the Hylleraas initial-state curve (dash-dotted line) and the Pluvinaage initial-state results (dashed line) have the same magnitude as the experimental data. Simply, changing the form of the final-state electron-electron Sommerfeld parameter to a complex number increased the overall magnitude of the FDCS by a factor of 250 and 100. Overall, the Hylleraas initial-state wave function results are in reasonably good agreement with the experimental data.

So far we have not included any initial- or final-state interactions between the projectile and the helium atom. As discussed in the Introduction, the relative velocities are in a regime where one would expect that the projectile should play an important role. To include the projectile interactions, we evaluate the full T-matrix [Eq. (3)] using the complete 6DW final-state wave function, and also including the CC approximation for the bound electron-free electron Coulomb interaction. We evaluate the full nine-dimensional integral without resorting to any simplifying approximations beyond those inherent in the general form of the final-state wave function. Two 6DW calculations are presented in Fig. 5. The solid curve is the 6DW (HY, CC), where the fully correlated 20 parameter Hylleraas wave function of Eq. (7) has been

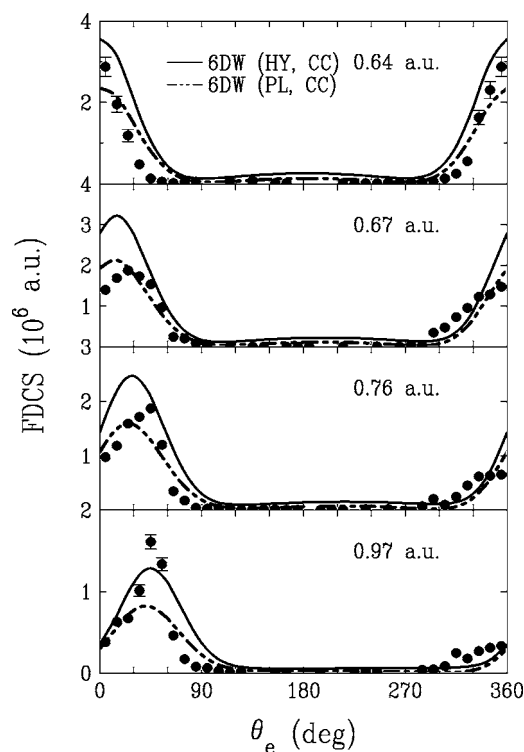


FIG. 5. Same kinematical conditions as Fig. 1, the solid circles are the absolute measurements and the theoretical curves are dashed-dotted line 6DW (HY, CC) model, and the short-dash long-dashed line 6DW (PL, CC) model.

used for the initial-state of the helium atom. The long dash-short-short curve is the 6DW (PL, CC) model where the initial-state helium wave function is the Pluvinaige wave function [Eq. (9)]. Allowing the projectile to interact with the target atom to all orders in the final state improves the agreement between experiment and theory as compared to the FBA (HY, 3C) and FBA (PL, 3C) results of Fig. 4. One of the noticeable effects for the projectile interactions is the reduction of the size of the recoil peak which is consistent with the experimental data. Also the 6DW models are in much more satisfactory agreement with experiment than the 3DW results of Fig. 1. It is difficult to determine the “best” initial-state choice from Fig. 5. The shape of the two different FDCS results in Fig. 5 are approximately the same, and the magnitudes differ by approximately a factor of 1.5. For the smallest and largest momentum transfers, the Hylleraas results are perhaps better and for the middle two cases in Fig. 5, the Pluvinaige results are perhaps better. Additional experimental results that probe the initial- and final-state correlation would be helpful.

#### IV. CONCLUSIONS

The primary objective of the present paper was to determine the role of the passive electron in the collision process. We have presented FDCS results using both an effective three-body (3DW) model for which the passive electron does not participate in the collision directly and two different four-body models [FBA (IS, FS) and 6DW (IS, FS)] for which the passive electron participates equally with the active electron. The shape of 3DW model results was in reasonable agreement with experiment but the magnitude was a factor of 4 too large compared to the absolute measurements. When we allowed the passive electron to participate on an equal footing, it was found that the treatment of the final-state interaction between the bound and ejected electrons could change the magnitude of the FDCS by orders of magnitude. We tried three different approximations for treating the final-state electron-electron interaction and found that the complex charge method of [34] gave results which had the same magnitude as the experimental data. The results were much less sensitive to the treatment of the initial state correlation between the two electrons (factor of 1.5 difference between Hylleraas and Pluvinaige wave functions). We are not persuaded that using the complex effective charge is necessarily the optimum way to treat the final-state electron-electron correlation. The important outcome of this work, though, lies in the fact that the FDCS results are extremely sensitive to how this interaction is treated and that the second electron seems to play an important role.

Despite the initial-state wave function controversy surrounding double ionization of a helium atom by electron impact, the present results do not decisively suggest which initial-state treatment of electron-electron correlation is better. We tried three different wave functions: (1) a 20 parameter Hylleraas wave function that yields a very accurate ground-state energy for helium but does not satisfy the Kato cusp condition; (2) the three parameter Le Sech wave function that satisfies the Kato cusp condition requirement and yields the ground-state energy to within three significant digits; and (3) the Pluvinaige wave function that satisfies the Kato cusp condition. The Hylleraas and Le Sech wave functions gave almost the same FDCS. The Hylleraas and Pluvinaige wave functions gave FDCS results that differed in magnitude by about 1.5 and it was not clear which one was in better agreement with experiment. Additional experimental results would be very valuable for examining the important physical effects contained in the initial- and final-state interactions.

- [1] A. T. Stelbovics, *Phys. Rev. Lett.* **83**, 1570 (1999).  
 [2] T. N. Rescigno, M. Baertschy, W. A. Isaacs, and C. W. McCurdy, *Science* **286**, 2474 (1999).  
 [3] S. Jones, D. H. Madison, A. Franz, and P. L. Altick, *Phys. Rev. A* **48**, R22 (1993).

- [4] D. S. F. Crothers and L. J. Dubé, *Adv. At., Mol., Opt. Phys.* **30**, 287 (1993).  
 [5] S. Jones and D. H. Madison, *Phys. Rev. A* **62**, 042701 (2000).  
 [6] M. Schulz, R. Moshhammer, A. N. Perumal, and J. Ullrich, *J. Phys. B* **35**, L161 (2002).

- [7] M. Foster, D. H. Madison, J. L. Peacher, M. Schulz, S. Jones, D. Fischer, R. Moshhammer, and J. Ullrich, *J. Phys. B* **37**, 1565 (2004).
- [8] M. Schulz, R. Moshhammer, D. Fischer, H. Kollmus, D. H. Madison, S. Jones, and J. Ullrich, *Nature (London)* **422**, 48 (2003).
- [9] M. Schulz, R. Moshhammer, A. N. Perumal, and J. Ullrich, *J. Phys. B* **35**, L161 (2002).
- [10] V. D. Rodriguez, *Nucl. Instrum. Methods Phys. Res. B* **205**, 498 (2003).
- [11] M. Foster, D. H. Madison, J. L. Peacher, and J. Ullrich, *J. Phys. B* **37**, 3797 (2004).
- [12] J. Fiol and R. E. Olson, *Nucl. Instrum. Methods Phys. Res. B* **205**, 474 (2003).
- [13] N. V. Maydanyuk, A. Hasan, M. Foster, B. Tooke, E. Nanni, D. H. Madison, and M. Schulz, *Phys. Rev. Lett.* **94**, 24320 (2005).
- [14] S. Jones and D. H. Madison, *Phys. Rev. Lett.* **91**, 073201 (2003).
- [15] L. U. Ancarani, T. Montagnese, and C. Dal Cappello, *Phys. Rev. A* **70**, 012711 (2004).
- [16] K. V. Rodriguez and G. Gasaneo, *J. Phys. B* **38**, L259 (2005).
- [17] J. Berakdar, *Phys. Rev. Lett.* **85**, 4036 (2000).
- [18] J. Berakdar, J. S. Briggs, and H. Klar, *J. Phys. B* **26**, 285 (1993).
- [19] M. Inokuti, *Rev. Mod. Phys.* **43**, 297 (1971).
- [20] H. Bethe, *Ann. Phys.* **5**, 325 (1930).
- [21] B. H. Bransden and C. J. Joachain, *Physics of Atoms and Molecules*, 2nd ed. (Pearson Education Limited, Harlow, England, 2003), Chap. 7, Sec. 4 p. 316.
- [22] E. A. Hylleraas, *Z. Phys.* **54**, 347 (1929).
- [23] J. F. Hart and G. Herzberg, *Phys. Rev.* **106**, 79 (1957).
- [24] C. Le Sech, *J. Phys. B* **30**, L47 (1997).
- [25] P. Pluvinage, *Ann. Phys.* **5**, 145 (1950).
- [26] S. Jones and D. H. Madison, *Phys. Rev. Lett.* **81**, 2886 (1998).
- [27] P. J. Redmond (unpublished), as discussed in L. Rosenberg, *Phys. Rev. D* **8**, 1833 (1973).
- [28] C. R. Garibotti and J. E. Miraglia, *Phys. Rev. A* **21**, 572 (1980).
- [29] D. S. F. Crothers and J. F. McCann, *J. Phys. B* **16**, 3229 (1983).
- [30] M. Brauner, J. S. Briggs, and H. Klar, *J. Phys. B* **22**, 2265 (1989).
- [31] J. R. Götz, M. Walter, and J. S. Briggs, *J. Phys. B* **38**, 1569 (2005).
- [32] D. P. Dewangan and B. H. Bransden, *J. Phys. B* **15**, 4561 (1982).
- [33] D. P. Dewangan, *J. Phys. B* **16**, L595 (1983).
- [34] D. Crothers and R. McCarroll, *Proc. Phys. Soc. London* **86**, 753 (1965).
- [35] B. Nath, R. Biswas, and C. Sinha, *J. Phys. B* **29**, 5909 (1996).